Supporting Information for

Unblocking the Potential of Ni-Based Metallic Glasses for Glucose Sensing Through Surface Porous Engineering

Lan Tan, Zhongzheng Yao, Jingqian Huang, Yu Lou, Yiming Zhao, Xindong Zhu, Sinan Liu, Jianrong Zen*, He Zhu*, Si Lan*

*Corresponding author. Email: zengjianrong@sinap.ac.cn (J. R. Z.); hezhu@njust.edu.cn (H. Z.); lansi@njust.edu.cn (S. L.)

Supplementary Figures

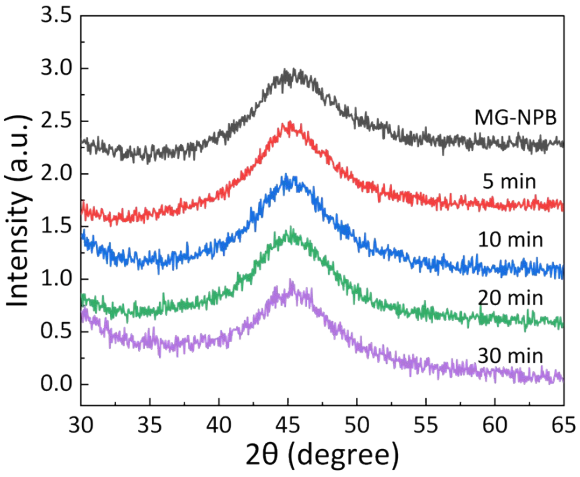

Figure S1. XRD patterns of $FeCl_3$-etched samples for different times (5, 10, 20, and 30 minutes).

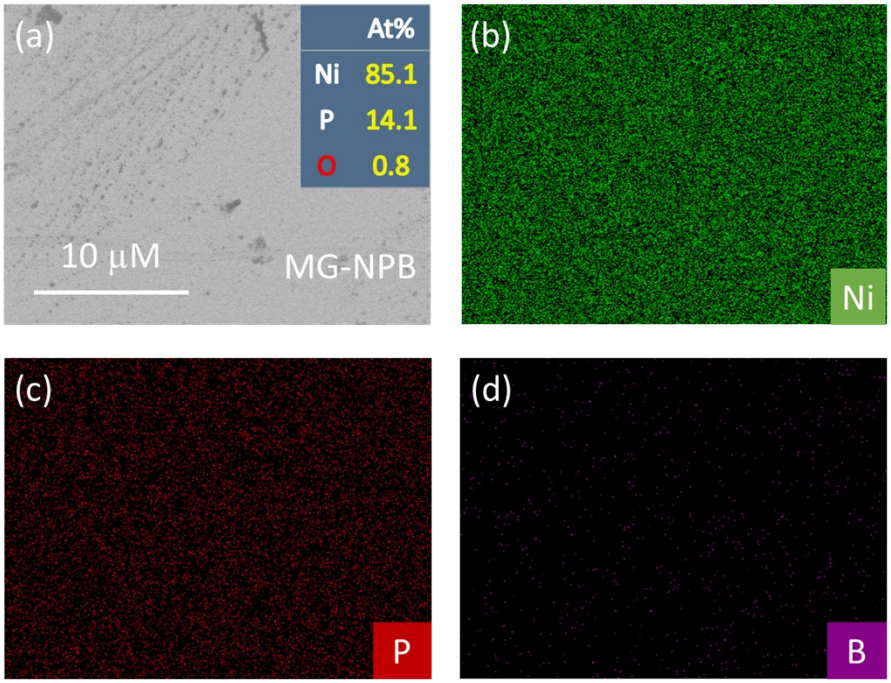

Figure S2. The SEM images of MG-NPB (insets: EDS quantitative measurements). (b-d) The EDS mapping images for (b) Ni, (c) P and (d) B on the surface of MG-NPB.

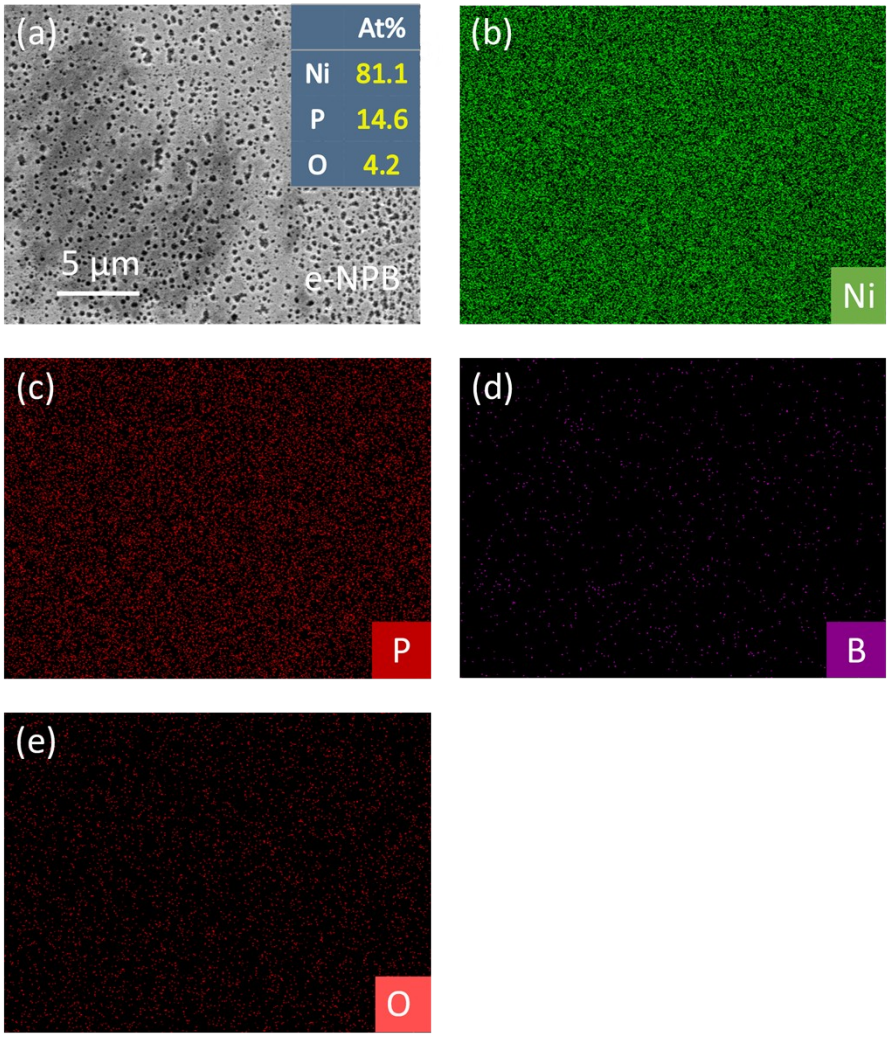

Figure S3. (a) The SEM images of e-NPB (insets: EDS quantitative measurements). (b-d) The EDS mapping images for (b) Ni, (c) P, (d) B and (e) O on the surface of e-NPB.

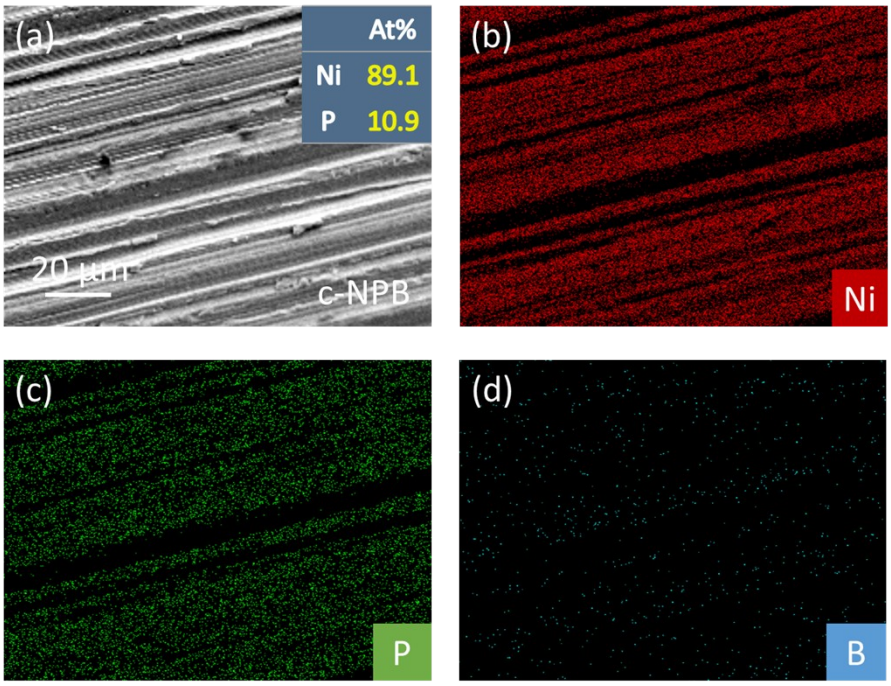

Figure S4. The SEM images of c-NPB (insets: EDS quantitative measurements). (b-d) The EDS mapping images for (b) Ni, (c) P and (d) B on the surface of c-NPB.

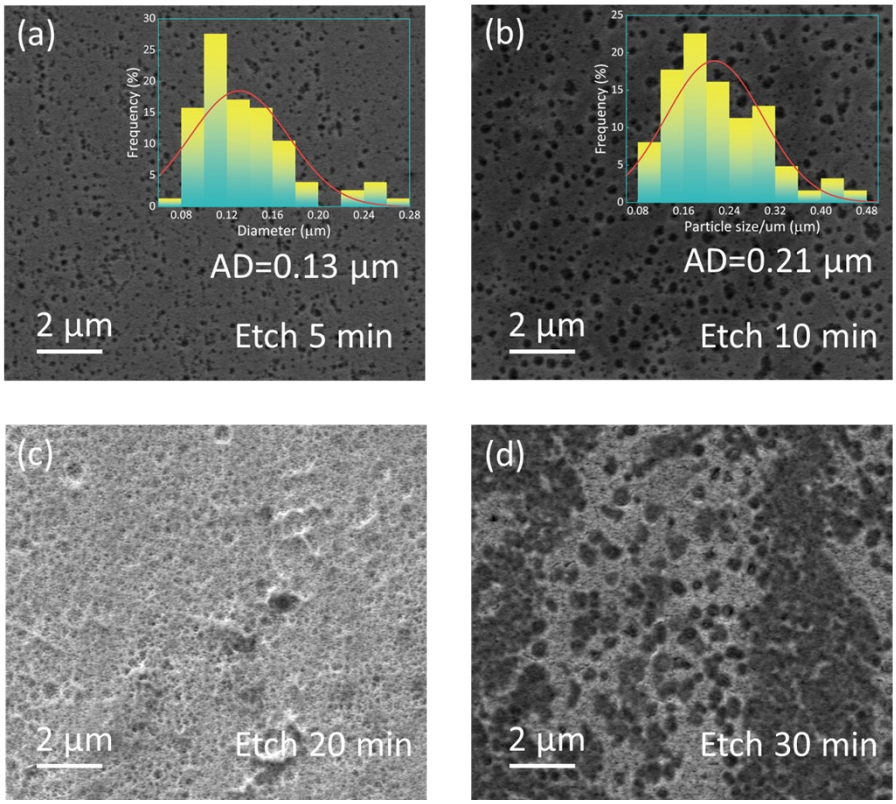

Figure S5. The SEM images of MG-NPB after immersing into $FeCl_3$ solution for (a) 5 min, (b) 10 min, (c) 5 min, (d) 30 min. The insets show the hole diameters distribution and the average values of the samples, measured statistically by Nano Measurer.

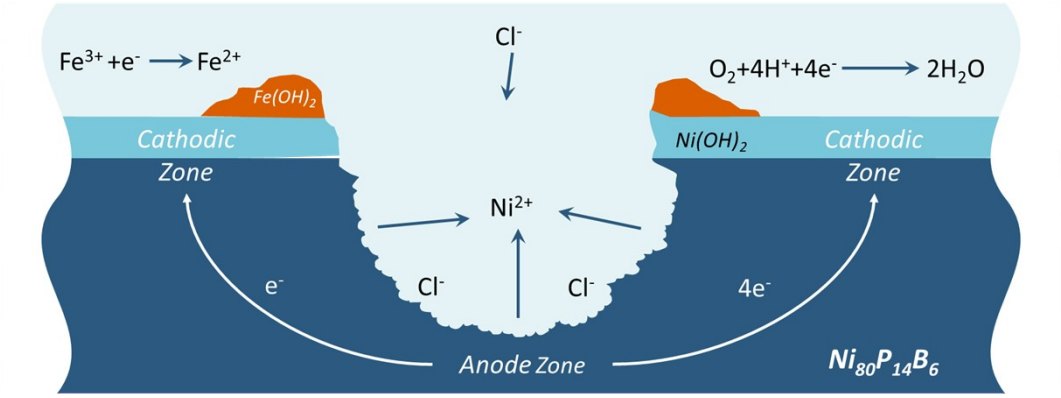

Figure S6. The schematic illustration of the chemical etching mechanism on the MG-NPB surface.

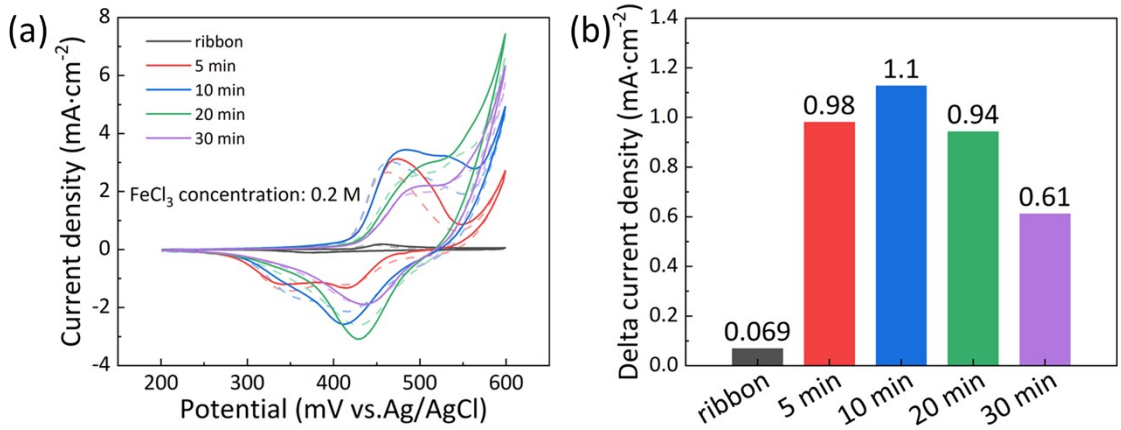

Figure S7. (a) CV curves of the MG-NPB with various etching times in 0.1 M NaOH solution with (solid line) or without (dotted line) glucose. (b) Maximum delta current density of the corresponding MG ribbons.

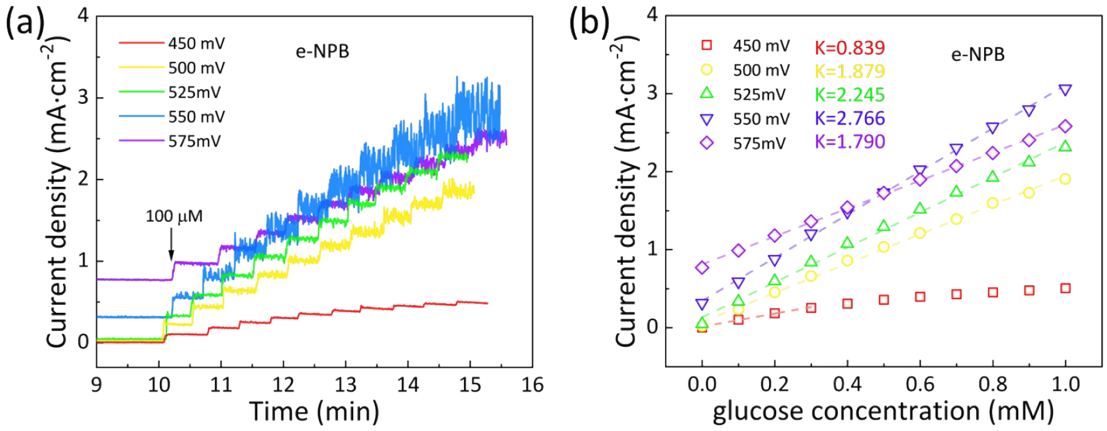

Figure S8. The i-t curves of e-NPB at various potential to the varied glucose concentration. (b) Linear fits of current density versus glucose concentration.

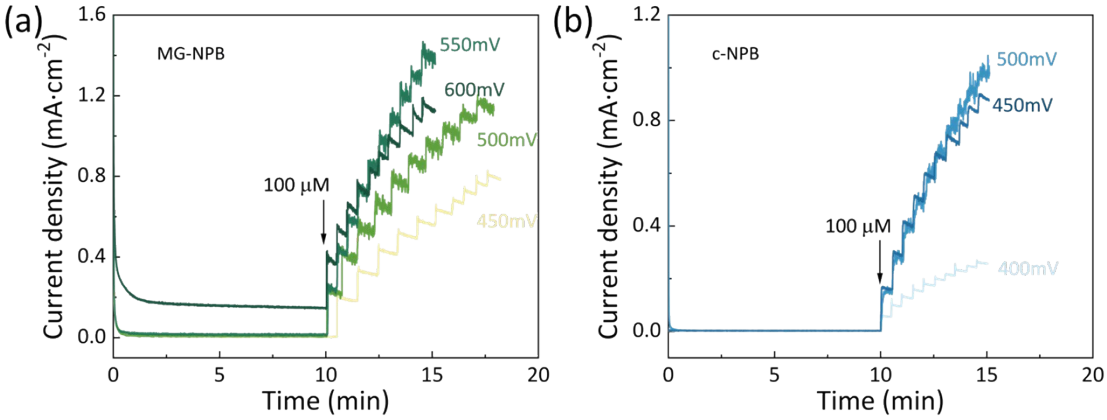

Figure S9. The i-t curves of (a) MG- and (b) c- NPB at various potential to the varied glucose concentration.

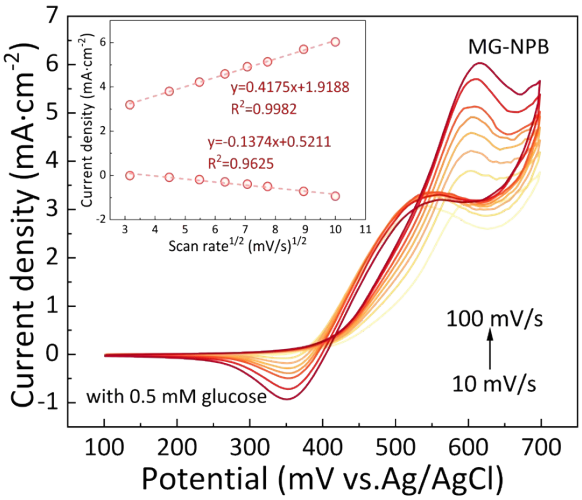

Figure S10. The CV curves of MG-NPB at various scan rates in 0.1 M NaOH with 0.5 mM glucose. The insets show the corresponding plots of I_{pa}-$\nu^{1/2}$ and I_{pc}-$\nu^{1/2}$ (I_{pa} and I_{pc} are the peak currents of the anode and cathode peaks, respectively).

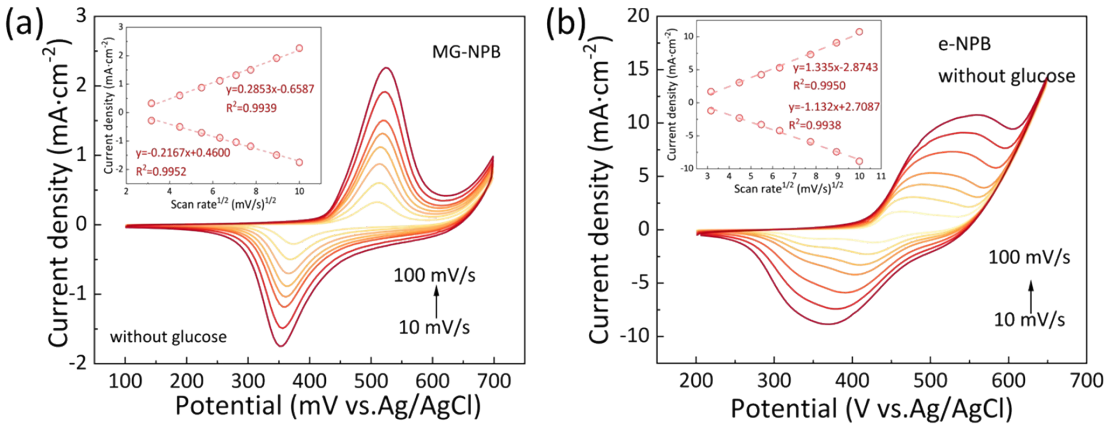

Figure S11. The CV curves of (a) MG-NPB and (a) e-NPB at various scan rates in 0.1 M NaOH without glucose. The insets show the corresponding plots of I_{pa}-$\nu^{1/2}$ and I_{pc}-$\nu^{1/2}$ (I_{pa} and I_{pc} are the peak currents of the anode and cathode peaks, respectively).

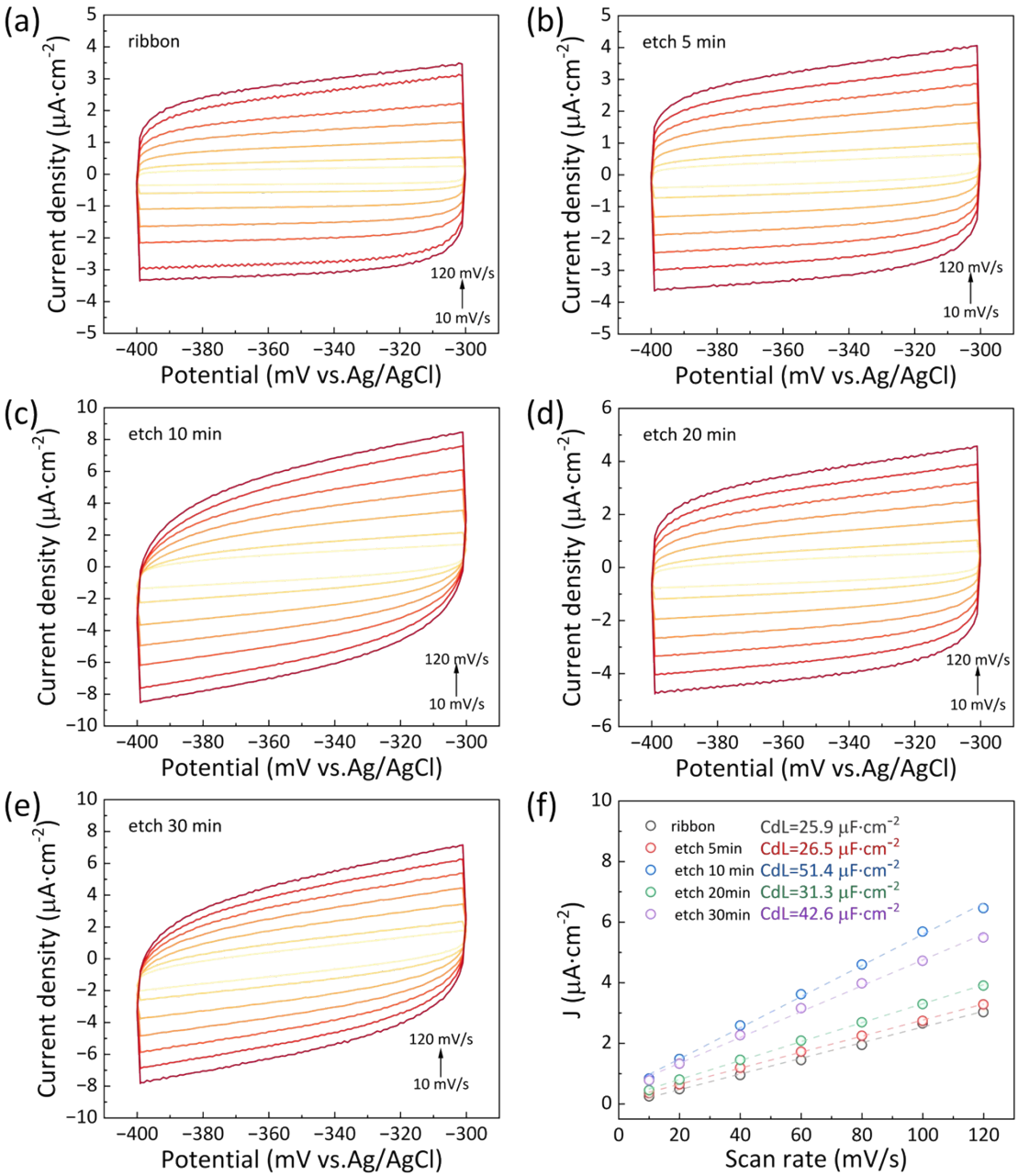

Figure S12. (a-e) CV curves recorded at non-Faradic potential window: (a) MG-NPB and (b-e) of MG-NPB etched at different time. The scan rate was from 10 to 120 mV/s. (f) Capacitive current density difference versus scan rates recorded at non-Faradic potential window.

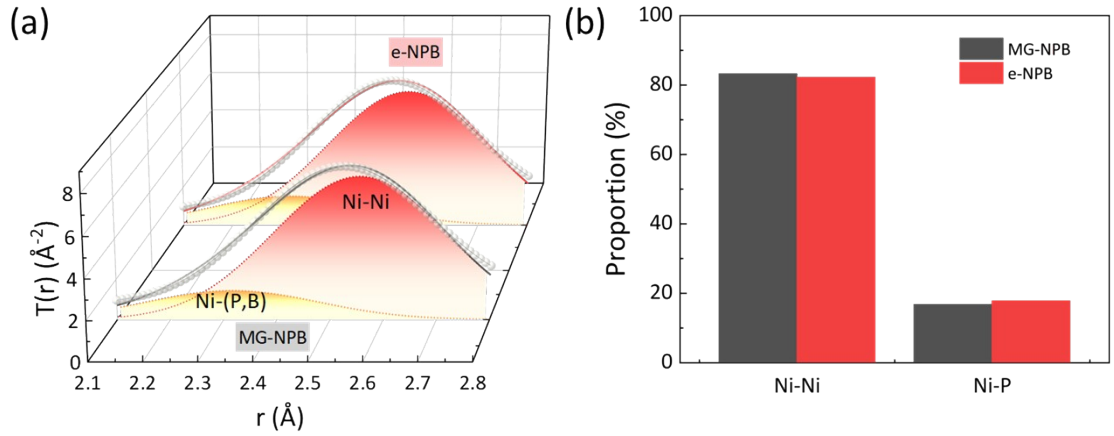

Figure S13. Synchrotron X-ray PDF study of MG-NPB before and after etching. (a) The fitted results of the first peak of T(r). (b) Mathematical statistics of atomic bonds.

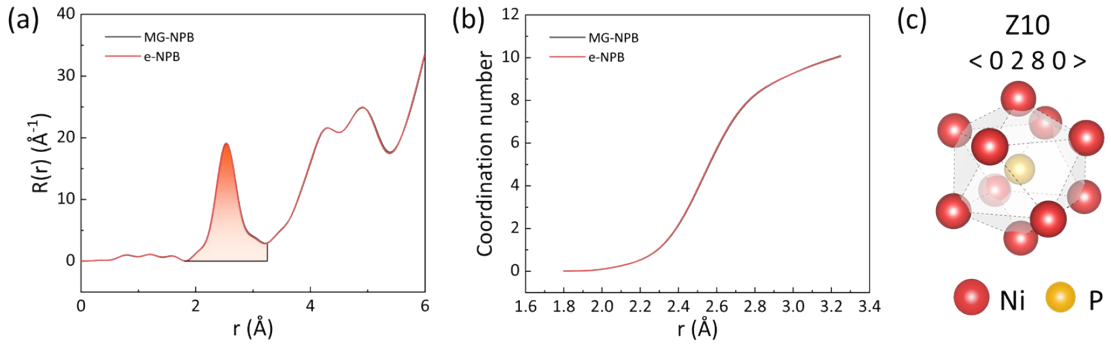

Figure S14. (a) Comparison of R(*r*) patterns for MG- and e-NPB samples. (b)The integrated area of the nearest-neighbor coordination shell of the radial distribution function profiles. (c) The Z10 icosahedral cluster structure.

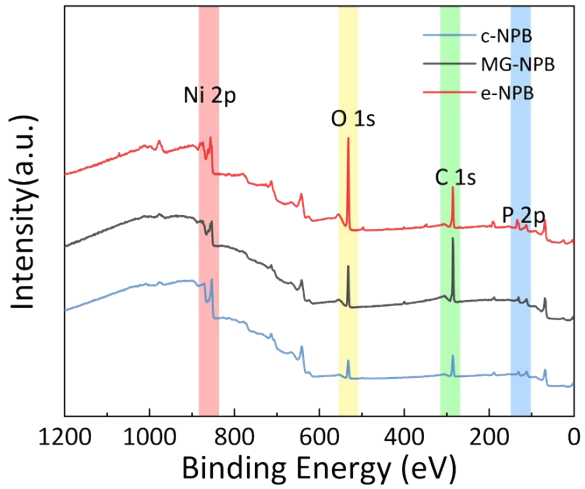

Figure S15. XPS survey scan of c-, MG- and e-NPB.

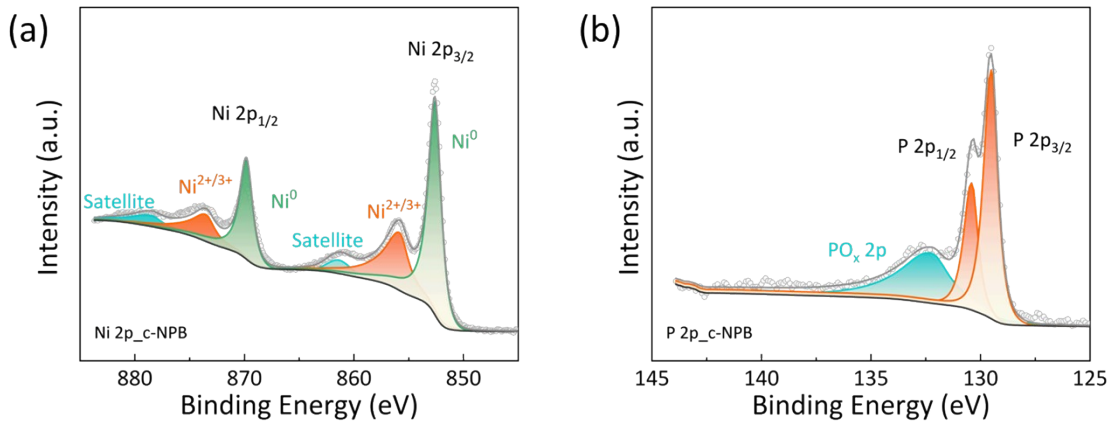

Figure S16. (a) Comparison of Ni 2p and (b) P 2p XPS spectra for c-NPB.

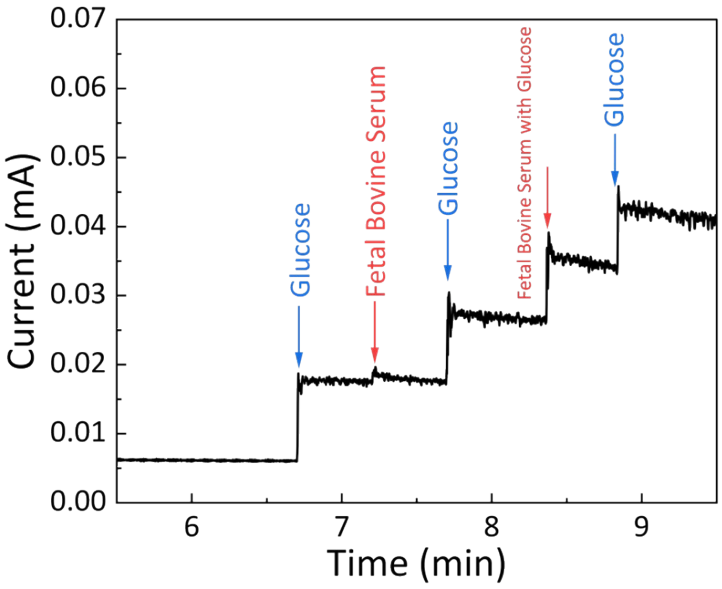

Figure S17. The i-t curves of e-NPB electrodes after successive additions of glucose or fetal bovine serum (in the order of 0.05 mM glucose, fetal bovine serum, 0.05 mM glucose, fetal bovine serum solution with 0.05 mM glucose, and 0.05 mM glucose).

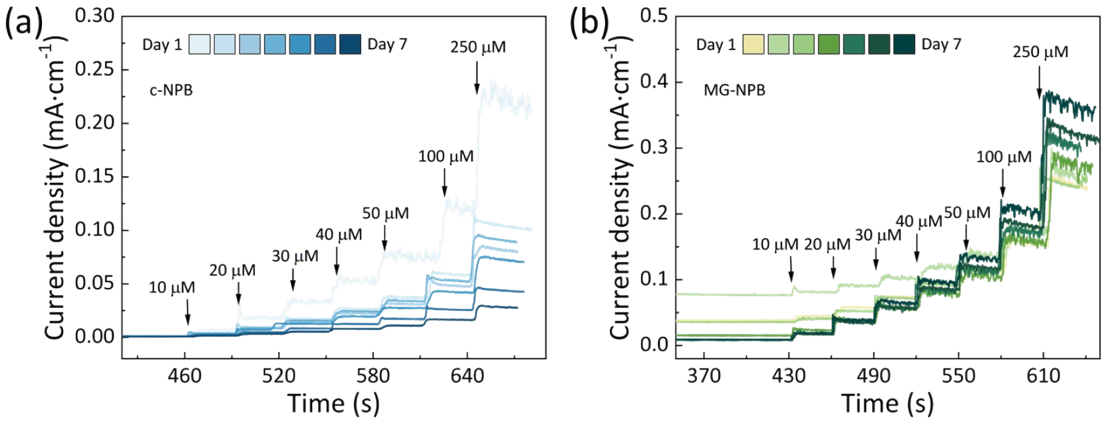

Figure S18. Repeatability of (a) c-NPB and (b) MG-NPB electrode across glucose concentrations between 1 and 500 µM in 0.1 M NaOH.

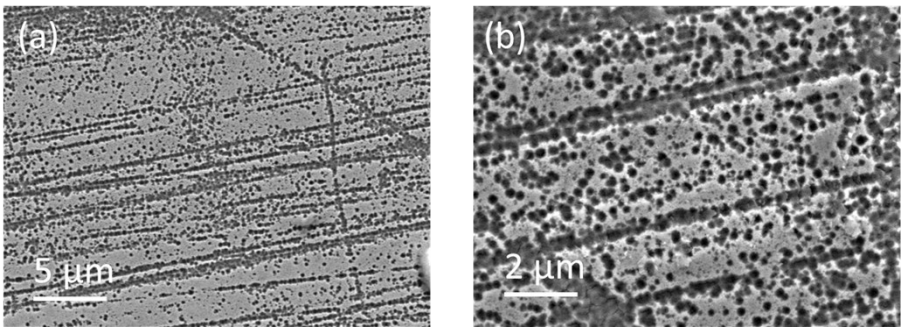

Figure S19. The SEM images of e-NPB after Repeatability test.

Supplementary Tables

Table S1. BET surface area c-, MG- and e-NPB.

	BET surface area (m^2/g)
c-NPB	0.3059
e-NPB	8.8542
MG-NPB	1.8936

Table S2. Fitting analysis of EIS of MG- and e-NPB.

	$R_s(\Omega)$	$R_{ct}(\Omega)$
MG-NPB	33.54	4429
e-NPB	35.84	311.6

Table S3. Fitting parameters of the peak fit for T(r) first peaks of MG- and e-NPB.

i-j	R_{ij} (Å)	W_{ij}	r_{ij} (Å)
Ni-Ni	2.56	0.816407195	2.56
Ni-P	2.28	0.152525203	2.267511961
Ni-B	2.18	0.02176549	
P-P	2.00	0.007123877	1.975023922
P-B	1.9	0.002033168	
B-B	1.8	0.000145067	

Table S4. Comparison of e-NPB catalyst performance with those recently reported in the literatures for glucose detection.

Electrode	Sensitivity ($\mu A \cdot mM^{-1} \cdot cm^{-2}$)	Linear range (mM)	Detection limit (mM)	Stability	Ref.
β-$Ni(OH)_2$/NP-Ni/MG	1218; 1496	0.045-5.665; 1-18	0.35	30 days, 96.83%	1
Ni-Co-Fe hydroxide/graphite sheet	1920.1; 1335.5	0.00025-0.4; 0.4-1	0.013	90 days, 104%	2
NiSA/NC	799.43	0.0008-1.124	0.22	--	3
NiCo-LDH@Ni-NTNW	4600; ~3300	0.03-1.05; 1.05-2.52	0.2	--	4
Amorphous Co-Ni hydroxide	1911.5; 1397.5	0.00025-1; 1-5	0.127	60 days, 102%	5
$Ni_{0.31}Co_{0.69}S_2$/rGO	1753; 954.7	0.001-55; 5-16	0.078	1 month, 91.6%	6
$CoMn_2O_4$@$Ni(OH)_2$	6.46; 4.46	0.0085-0.0705; 0.0705-1.8305	0.264	21 days, 93.6%	7
Ni/$rGO_{0.2}$/PP	1120; 1230	0.0005-0.006; 0.1-1	0.36	--	8
Ni/Co-MOF	2086.7	0.0001-1.4	0.047	--	9
Cu_xO@Cu	1600	0.02-10	7.3	25 days, 93%	10
e-NPB	2637; 1679	0.01-1; 1-5	2.82	7 days, 116%	This work

Reference:

1 Y. Zhang, D. Zheng, S. Liu, S. Qin, X. Sun, Z. Wang, C. Qin, Y. Li and J. Zhou, *Applied Surface Science*, 2021, **552**, 149529.

2 H. B. Li and P. Zhao, *Journal of Alloys and Compounds*, 2019, **800**, 261-271.

3 H. Yin, X. Bai and Z. Yang, *Chemical Engineering Journal*, 2023, **478**, 147510.

4 K. M. Amin, F. Muench, U. Kunz and W. Ensinger, *Journal of Colloid and Interface Science*, 2021, **591**, 384-395.

5 H. Li, L. Zhang, Y. Mao, C. Wen and P. Zhao, *Nanoscale Research Letters*, 2019, **14**, 135.

6 G. Li, H. Huo and C. Xu, *Journal of Materials Chemistry A*, 2015, **3**, 4922-4930.

7 X. Wang, L. Hao, R. Du, H. Wang, J. Dong and Y. Zhang, *Journal of Colloid and Interface Science*, 2024, **653**, 730-740.

8 Z. Li, Z. Chen, X. Ji, H. Jin, Y. Si, J. Zhang, C. Chen and D. He, *Nano Research*, 2024, **17**, 6258-6264.

9 H. Zou, D. Tian, C. Lv, S. Wu, G. Lu, Y. Guo, Y. Liu, Y. Yu and K. Ding,

Journal of Materials Chemistry B, 2020, **8**, 1008-1016.
10 J. Wen, S.-Q. Chen, X. Wu, B. Li, H. Peng, T. Feng and S. Lan, *Journal of Alloys and Compounds*, 2025, **1011**, 178337.